4-16-2020

Numerical Simulation of the Nagumo Equation by Finite Difference Method

Gabriel Garcia

NUMERICAL SIMULATION OF THE NAGUMO EQUATION BY FINITE DIFFERENCE METHOD

A Thesis

by

GABRIEL PERRY NATANNI GARCIA

Submitted to Texas A&M International University
in partial fulfillment of the requirements
for the degree of

MASTER OF SCIENCE

December 2015

Major Subject: Mathematics

NUMERICAL SIMULATION OF THE NAGUMO EQUATION BY FINITE DIFFERENCE METHOD

NUMERICAL SIMULATION OF THE NAGUMO EQUATION BY FINITE DIFFERENCE METHOD

A Thesis

by

Gabriel Perry Natanni Garcia

Submitted to Texas A&M International University
in partial fullfillment of the requirements
for the degree of

MASTER OF SCIENCE

Approved as to style and content by:

Chair of Committee,	Runchang Lin
Committee Members,	Rohitha Goonatilake
	Qingquan Wu
Head of Department,	Rohitha Goonatilake

December 2015

Major Subject: Mathematics

ABSTRACT

Numerical Simulation of the Nagumo Equation by Finite Difference Method (December 2015)

Gabriel Perry Natanni Garcia, B.S., Texas A&M University;

Chair of Committee: Dr. Runchang Lin

The Nagumo equation is an important nonlinear reaction-diffusion equation used to model the transmission of nerve impulses. In this thesis, traveling wave solutions to the Nagumo equation are studied. A pseudo-Crank-Nicolson finite difference scheme is developed to find numerical solutions. The exact solution of Kawahara and Tanaka is used to demonstrate the efficiency of the scheme. It is confirmed that the numerical errors, evaluated in the discrete maximum norm, converge in $O(\Delta x^2 + \Delta t)$, where Δx and Δt are spatial and temporal step sizes, respectively. More simulations with different initial conditions are conducted. In particular, it is observed that the amplitude of the impulse is the major factor in determining if the wave damps down to the resting or rises to the excited state. For values $u(x, 0) \leq \alpha$, the wave approaches the 0 resting state and for $u(x, 0) > \alpha$ the wave rose to the 1 excited state.

ACKNOWLEDGMENTS

I would like to thank my thesis advisor, Dr. Runchang Lin, and advisory committee members, Dr. Rohitha Goonatilake, and Dr. Qingquan Wu for their guidance and support throughout the course of this research and my academic career. Thanks also go to my friends, colleagues, and the rest of the department faculty and staff for making my time at Texas A&M International University an enjoyable and enriching experience. Finally, a special thank you to my family for their patience, love, and support. Also, I gratefully acknowledge the support from the NSF through the grant DMS #117268.

TABLE OF CONTENTS

LIST OF TABLES

Page

LIST OF FIGURES

CHAPTER I

INTRODUCTION

As computers advance, the ability to implement more detailed and complex mathematical models advances as well. Therefore, the increase in the study of non-linear partial differential equations. More and more mathematical models are used to simulate real world phenomena using mathematical properties. Though mathematical models do not incorporate every feature of real world phenomena, they still provide useful information.

In this thesis, the focus is on the application of mathematical modeling in the field of neurophysiology. Particularly, the transmission of electrical pulses by tiny nerve cells called neurons. Neurons differ in size, shape, and are classified into different types based on certain features. Three main features of a neuron are dendrites, a soma, and axon. The axon of the neuron is the medium used to transport the electrical signals to neighboring neurons. These electrical signals are known as an action potential.

The generation of an action potential is largely governed by the transportation of sodium, Na^+, and potassium, K^+, ions through the cell membrane. During the resting state, the cytoplasm inside the axon contains an ionic composition that makes the cell membrane's interior slightly negative than the exterior. This potential difference is typically -70mV, and maintained by activation gates of the voltage-gated Na^+ and K^+ channels being closed, but the inactivation gate of the Na^+ channel remains open. When an outside stimulus is applied, the cell membrane becomes more positive than the resting state. This stimulus needs to meet a threshold voltage in order to generate an action potential. If the voltage is less than the threshold voltage, then the cell membrane will remain at the resting potential, but if the stimulus is greater than the threshold voltage the Na^+ activation gates open up. This is the all or none principle. The Nagumo equation models this principle. For a more detailed description on all the mechanisms generating an action potential, please refer to [22].

The thesis begins with well-known historical developments of the action potential. Furthermore, the existence and uniqueness criteria of solutions to the Nagumo equation is proved, and it is shown they can be traveling waves. Then a description of the finite difference method, which is used to develop a numerical scheme to find numerical solutions. These numerical solutions are then compared with the exact solution and analysis is carried out to verify the efficiency of the numerical scheme. Following verification, more examples are ran with different initial conditions for the Nagumo equation.

This thesis follows the style of the *SIAM Journal on Numerical Analysis*.

CHAPTER II

BACKGROUND

In 1902, Julius Bernstein hypothesized that the negative charge in the interior of the cell membrane was due to the permeability of K^+ ions [21]. Bernstein proposed that the excitation caused by a stimulus increased the permeability of the cell membrane to all ions. This caused the membrane potential to drop to zero and generated an action potential equal in absolute size to the resting potential, but in the opposite direction.

In the 1930s, research conducted by K.S. Cole and Howard Curtis confirmed Bernstein's hypothesis that a stimulus to the cell membrane increased the permeability to more ions [4]. There experiments were one of the first to implement the voltage clamp technique. This technique permitted the experimenter to keep the cell membrane's potential at a set level. Their findings showed the electrical capacitance of the cell membrane during an action potential did not change, but a drop in the resistance was reported. This drop in resistance is attributed to the cell membrane's increase in permeability to ions.

In 1952, A.L Hodgkin and A.F. Huxley developed a mathematical model of th nerve cell's behavior in a giant squid axon using the voltage clamp technique. Their work confirmed and added to Bernstein's early hypothesis of the cell membrane's permeability, in which it was not only permeable to K^+, but to Na^+ as well. Their model consisted of four ordinary differential equations.

In 1961, Richard Fitzhugh simplified the Hodgkin-Huxley (HH) model from four to two ordinary differential equations [9]. Fitzhugh's work focused on a modified version of the Van der Pol model to explain the basic properties of excitability of the HH model. A year later Nagumo et al. [18] [19] developed the equivalent circuit that possessed the same basic properties of excitability the Fitzhugh's model presented.

In the next section, we will examine the characteristics of the HH model and Fitzhugh-Nagumo (FN) model.

2.1 . HODGKIN-HUXLEY MODEL

Mathematical models of action potentials are classified into two types: quantitative and qualitative. This section analyzes the quantitative model developed by Hodgkin and Huxley. The HH model is considered quantitative, since it reflected their experimental data. Their model, as proposed in their fifth paper [11], is based on the idea that an electrical circuit can model the electrical properties of the cell membrane. Murray gives a detailed derivation into the equations that govern the HH model [17].

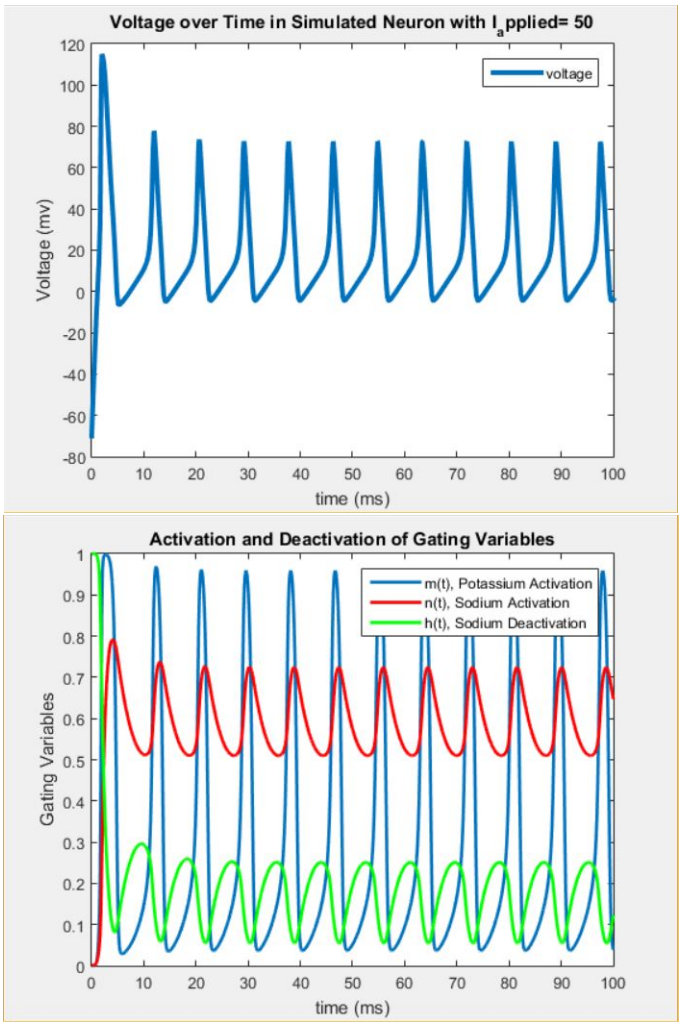

FIGURE 2.1. *Action potential and gating variables for HH model with stimulus of 50 mV.*

The HH model is

$$
\begin{aligned}
C\frac{dv}{dt} &= g_{Na}m^3h(V - V_{Na}) + g_K n^4 h(V - V_k) + g_L(V - V_L),\\
\frac{dm}{dt} &= \alpha_m(V)(1 - m) - \beta_m(V)m,\\
\frac{dh}{dt} &= \alpha_h(V)(1 - h) - \beta_h(V)h,\\
\frac{dn}{dt} &= \alpha_n(V)(1 - n) - \beta_n(V)n.
\end{aligned}
$$

The variables m, n, and h are variables bounded by 0 and 1, and the values for α and β are the values Hodgkin and Huxley fitted their data with by using exponentials [11]. Figure 2.1 is a simulation of the HH model with parameters from their 1952 paper.

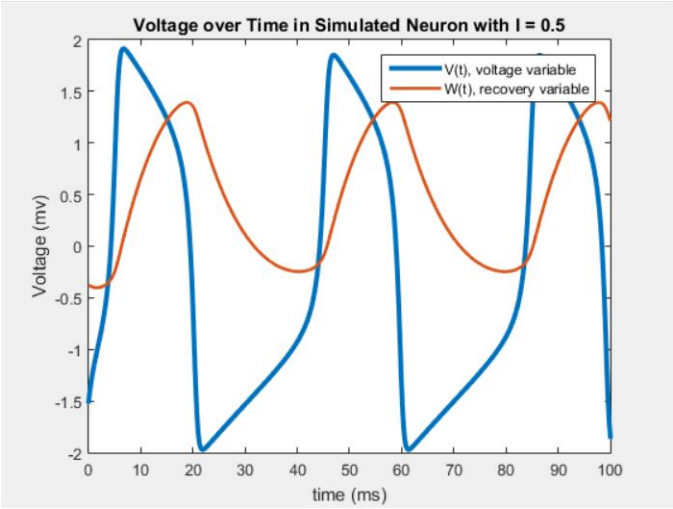

FIGURE 2.2. *FN model with constant oscillation of action potential.*

2.2 . FITZHUGH-NAGUMO MODEL

The FN model consists of two variables, one fast, v, and one slow, r. The variable v is dependent and corresponds to the rate of change of neuron membrane potential with respect to time. It is similar to the V and m of the HH model. The r variable is known as the recovery variable. The variable r simulates the h and n of the HH model. The FN model (see [3] [8] [9] [14] for more details) is

$$\frac{\partial v}{\partial t} = \frac{\partial v}{\partial x^2} + v(1-v)(v-\alpha) - r,$$
$$\frac{\partial r}{\partial t} = \epsilon(v - \gamma r)$$

where $0 < \alpha < 1$. Figure 2.2 is a simulation of the FN model.

2.3 . NAGUMO EQUATION

From the FN model, the Nagumo equation is derived by setting the recovery variable r equal to zero. This gives the Nagumo equation [16] as

$$\frac{\partial u}{\partial t} = \frac{\partial u}{\partial x^2} + u(1-u)(u-\alpha), \tag{2.1}$$

where $0 < \alpha < \frac{1}{2}$, $x \in \Re$, and $t \geq 0$. The Nagumo equation is an important nonlinear reaction-diffusion equation. The Nagumo equation is particularly useful as a model of the transmission of nerve impulses and in population genetics [1]. Green and Sleeman give a physiological interpretation to the FN model in [10] that can be applied to the Nagumo equation. For the Nagumo equation, u represents the potential difference between the interior and exterior of the cell membrane. The nonlinear term in (2.1) is analogous to an

instantaneous turning of sodium permeability above the threshold voltage α.

CHAPTER III

EXISTENCE OF TRAVELING WAVE SOLUTIONS

In this chapter, solutions to the Nagumo equation are shown to exist and are unique. Furthermore, the development of traveling wave solutions to the Nagumo equation (2.1) is given.

3.1 . EXISTENCE AND UNIQUENESS

In order to show solutions to the Nagumo equation (2.1) existence and uniqueness, the mathematical problem needs to be defined.

DEFINITION 3.1. *Let $Q_T = \Omega \times (0,T)$, where Ω is a given bounded time-independent n-dimensional spatial domain with boundaries $S_0 = \Omega \times \{0\}$, $S_T = \Omega \times \{T\}$, and $\Gamma = \partial\Omega \times (0,T)$. Then the initial-boundary-value (IBV) problem is*

$$u_t - \nabla^2 u - f(u) = 0 \quad in \quad Q_T \cup S_T, \quad where \quad f(u) = u(1-u)(u-\alpha)$$

with initial conditions

$$u(x,0) = u_0(x) \quad in \quad S_0,$$

and boundary equations

$$u(x,t) = b(x,t) \quad in \quad \Gamma.$$

The Nagumo equation (2.1) is a special case of the IBV problem in Definition 3.1.

In proving the solutions existence and uniqueness, the following theorem from Britton [2] and definition are used:

THEOREM 3.2. *(Global Existence and Uniqueness): Let f be Lipschitz continuous. Let $f(a) \geq 0$, $f(b) \leq 0$, $-\infty < a < b < \infty$, and $u(x,0) \in \sum = \{u | a \leq u \leq b\}$ on S_0, and $Bu \in c\sum$ on Γ. Then there exists a unique solution of the initial-boundary-value problem for all time.*

DEFINITION 3.3. *A function f is Lipschitz continuous on a domain D, then there exists a constant $K > 0$ such that for all $x, y \in D$*

$$|f(x) - f(y)| \leq K|x - y|.$$

Now consider the IBV problem specified in Definition 3.1. Since $u(x,0)$ is the initial condition, it can be chosen such that $u(x,0) \in \sum = \{u | a \leq u \leq b\}$ on S_0. For the purposes of establishing existence and uniqueness, $a = 0$ and $b = 1$. The values for a and b are chosen such that $-\infty < a < b < \infty$ is met. Thus, the first condition is satisfied.

On the other hand, clearly

$$f(0) = 0(1-0)(0-\alpha) = 0 \geq 0.$$

and

$$f(1) = 1(1-1)(1-\alpha) = 0 \leq 0.$$

The next condition is to show $f(u)$ is Lipschitz continuous. By Definition 3.3, $f(u)$ needs to be differentiable and $|f'(u)|$ to be bounded. The $f(u)$ in Definition 3.1 is differentiable for all $u(x,t) \in (0,1)$ and $\alpha \in (0, \frac{1}{2})$. $|f'(u)|$ is bounded in $(0,1)$ by applying the mean value theorem. This gives

$$|f'(c)| = \frac{|f(1) - f(0)|}{|1-0|} = 0, \quad \text{where} \quad c \in (0,1) \quad \text{and} \quad 0 < c < 1.$$

By Theorem 3.2, solutions to the Nagumo equation exist and are unique.

3.2 . TRAVELING WAVE SOLUTIONS

In this section, the traveling wave solutions for the Nagumo equation (2.1) are developed. Note that the Nagumo equation has three steady states, which are 0, 1, and α.

A traveling wave solution is a solution of the form

$$u(x,t) = U(z), \tag{3.2}$$

where $z = x - ct$ and $c \geq 0$ is the wave speed.

Substituting (3.2) into (2.1) gives

$$-cU' = U(1-U)(U-\alpha) + U'', \tag{3.3}$$

where the prime denotes differentiation with respect to z, or

$$U'' + cU' + U(1-U)(U-\alpha) = 0. \tag{3.4}$$

A typical wave front solution is where U is at a steady state on both ends. This sets up an eigenvalue problem to determine the values of the wave speed c such that nonnegative solutions U exists that satisfies both

$$\lim_{z \to -\infty} U(z) = 0 \quad \text{and} \quad \lim_{z \to +\infty} U(z) = 1.$$

Now the solutions for U can be studied in the (U, V) phase plane by setting

$$dV = -cV - U(1-U)(U-\alpha) = F(U,V) \tag{3.5}$$

$$dU = V = G(U,V). \tag{3.6}$$

In order to find critical points, we need to find values for V and U, such that $dV = 0$ and $dU = 0$. In doing so, there are three critical points at (0,0), $(0, \alpha)$, and (0,1). Furthermore, if dV and dU are analytic near these critical points, then they can be expanded into their respected Taylor series. Then by retaining only the linear terms have

$$A = \begin{pmatrix} f_v & f_u \\ g_v & g_u \end{pmatrix} = \begin{pmatrix} -c & -3u^2 + 2u(1+\alpha) - \alpha \\ 1 & 0 \end{pmatrix} \tag{3.7}$$

Let $\lambda_\pm$ be the eigenvalues of the matrix defined in (3.7), which can be determined by taking $det(A - \lambda I) = 0$. Thus

$$det(A - \lambda I) = \begin{vmatrix} -c-\lambda & -3u^2 + 2(1+\alpha)u - \alpha \\ 1 & -\lambda \end{vmatrix} = 0 \Rightarrow \lambda_\pm = \lambda^2 - c\lambda + 3u^2 - 2(1+\alpha)u + \alpha. \tag{3.8}$$

For each critical point, their stability is determined from these eigenvalues. They are as follows:

$$(0,0): \quad \lambda_\pm = \frac{-c \pm \sqrt{c^2 - 4\alpha}}{2} \qquad \Rightarrow \begin{cases} \text{stable node} & \text{if } c^2 > 4\alpha \\ \text{stable spiral} & \text{if } c^2 < 4\alpha \end{cases} \tag{3.9}$$

$$(\alpha,0): \quad \lambda_\pm = \frac{-c \pm \sqrt{c^2 - 4(\alpha^2 - \alpha)}}{2} \quad \Rightarrow \text{saddle point} \tag{3.10}$$

$$(1,0): \quad \lambda_\pm = \frac{-c \pm \sqrt{c^2 - 4(1-\alpha)}}{2} \qquad \Rightarrow \begin{cases} \text{stable node} & \text{if } c^2 > 4(1-\alpha) \\ \text{stable spiral} & \text{if } c^2 < 4(1-\alpha). \end{cases} \tag{3.11}$$

Near each critical point, the solutions to the nonlinear equation can be approximated locally by

$$\begin{pmatrix} x \\ y \end{pmatrix} = c_1 v_1 e^{\lambda_+ t} + c_2 v_2 e^{\lambda_- t}, \tag{3.12}$$

where c_1 and c_2 are arbitrary constants and v_1, v_2 are the eigenvectors of A corresponding to λ_+ and λ_- respectively. The eigenvectors are given by

$$v_{1,2} = (1 + p_\pm^2)^{-\frac{1}{2}} \begin{pmatrix} 1 \\ p_\pm \end{pmatrix}, \quad p_\pm = \frac{\lambda_\pm + c}{-3u^2 + 2(1+\alpha)u - \alpha}, \quad \text{with} \quad -3u^2 + 2(1+\alpha)u - \alpha \neq 0. \tag{3.13}$$

CHAPTER IV

FINITE DIFFERENCE METHOD

The numerical approximation method used in solving the Nagumo equation is described in this section. In essence, the finite difference method attempts to solve partial differential equations by approximating the differential equation over the area of integration by a system of algebraic equations. The partial derivatives in equations will be replaced by quotients of differences. This allows for the development of an algebraic equation system.

For time dependent problems, people may use Explicit, Implicit, or Crank-Nicolson (CN) Method. Each of the individual methods differ in stability, accuracy, and execution of speed in their attempts to solve nonlinear partial differential equations.

4.1 . DIFFERENCE APPROXIMATIONS

In this section, for simplicity the difference approximations are going to be over $\Omega = [x_L, x_R]$ where $x_L < x_R$ and $t \in [0.T]$. Define $x_i = x_L + i\frac{x_R - x_L}{N} = x_L + i\Delta x$ for $0 \leq i \leq N$ and $t_n = n\frac{T}{M} = n\Delta t$ for $0 \leq n \leq M$. To start, the following approximation is valid for the derivative of f:

$$\frac{\partial f}{\partial x(x_i)} = \frac{f(x_i + \Delta x) - f(x_i - \Delta x)}{2\Delta x} = \frac{f_{i+1} - f_{i-1}}{2\Delta x}. \tag{4.14}$$

Then use Taylor series to get

$$f_{i+1} = f_i + \frac{\partial f}{\partial x(x_i)}\Delta x + \frac{\partial^2 f}{\partial^2 x(x_i)}\frac{(\Delta x)^2}{2!} + \frac{\partial^3 f}{\partial^3 x(x_i)}\frac{(\Delta x)^3}{3!} + \mathcal{O}(\Delta x^4) \tag{4.15}$$

and

$$f_{i-1} = f_i - \frac{\partial f}{\partial x_i}\Delta x + \frac{\partial^2 f}{\partial^2 x(x_i)}\frac{(\Delta x)^2}{2!} - \frac{\partial^3 f}{\partial^3 x(x_i)}\frac{(\Delta x)^3}{3!} + \mathcal{O}(\Delta x^4). \tag{4.16}$$

Since Δx is very small, higher order values can be neglected. These higher order values of Δx are the truncation error.

Rewriting (4.15), the forward difference approximation is

$$\frac{\partial f}{\partial x(x_i)} = \frac{f_{i+1} - f_i}{\Delta x} - \mathcal{O}(\Delta x). \tag{4.17}$$

When using the forward difference approximation the truncation error is of first order. Similarly, using (4.16) the backwards difference approximation is:

$$\frac{\partial f}{\partial x(x_i)} = \frac{f_i - f_{i-1}}{\Delta x} - \mathcal{O}(\Delta x). \tag{4.18}$$

In the backwards difference approximation, the truncation error is first order. Next, the central difference approximation is obtained by subtracting (4.16) from (4.15). This gives

$$\frac{\partial f}{\partial x(x_i)} = \frac{f_{i+1} - f_{i-1}}{\Delta x} - \mathcal{O}(\Delta x^2). \tag{4.19}$$

The truncation error for the central difference approximation is smaller, being of second order. To derive the second order spatial derivative, add (4.15) and (4.16). The central difference for second derivative is:

$$\frac{\partial^2 f}{\partial^2 x(x_i)} = \frac{f_{i+1} - 2f_i + f_{i-1}}{\Delta x} - \mathcal{O}(\Delta x^2). \tag{4.20}$$

Similarly, the truncation error is second order.

4.2 . METHODS

The finite difference form of the Nagumo equation is given with spatial second derivative evaluated from a combination of the derivatives at time steps n and n+1.

$$\frac{u_i^{n+1} - u_i^n}{\Delta t} = (\theta)\frac{u_{i+1}^n - 2u_i^n + u_{i-1}^n}{(\Delta x)^2} + (1-\theta)\frac{u_{i+1}^{n+1} - 2u_i^{n+1} + u_{i-1}^{n+1}}{(\Delta x)^2}. \tag{4.21}$$

From (4.21), the different types of finite difference methods for the Nagumo equation can be obtained depending on the value for θ. $\theta = 1$ is the explicit method, the implicit method for $\theta = 0$, and the CN method for $\theta = \frac{1}{2}$, respectively, as shown in (4.22), (4.23), and (4.24):

$$\frac{u_i^{n+1} - u_i^n}{\Delta t} = \frac{u_{i+1}^n - 2u_i^n + u_{i-1}^n}{(\Delta x)^2} + u_i^n(1 - u_i^n)(u_i^n - \alpha), \tag{4.22}$$

$$\frac{u_i^{n+1} - u_i^n}{\Delta t} = \frac{u_{i+1}^{n+1} - 2u_i^{n+1} + u_{i-1}^{n+1}}{(\Delta x)^2} + u_i^n(1 - u_i^n)(u_i^n - \alpha), \tag{4.23}$$

$$\frac{u_i^{n+1} - u_i^n}{\Delta t} = \frac{u_{i+1}^n - 2u_i^n + u_{i-1}^n}{2(\Delta x)^2} + \frac{u_{i+1}^{n+1} - 2u_i^{n+1} + u_{i-1}^{n+1}}{2(\Delta x)^2} + u_i^n(1 - u_i^n)(u_i^n - \alpha). \tag{4.24}$$

For our problem we are going to use a psuedo-CN method due to the nonlinear term in (4.24). Compared to the other two stated methods, the psuedo-CN method converges at a faster rate and has a smaller truncation error of $\mathcal{O}(\Delta x^2)$ and $\mathcal{O}(\Delta t)$. Fadugba et al. [6] and Saad Manna et al. [15] showed these two properties of the CN method in their work on the Heat equation and generalized Huxley equation, respectively.

4.3 . VON NEUMANN STABILITY

In this section, the stability of the psuedo-CN method is examined. By examining the stability, it is ensured that the errors in the method do not grow causing the method to blow up. To examine this, the Von Neumann technique of stability analysis is utilized.

The first step to carry out this technique is to linearize the nonlinear term by making it locally constant. In doing so, (4.24), takes the form

$$\frac{u_i^{n+1}-u_i^n}{\Delta t}=\frac{u_{i+1}^n-2u_i^n+u_{i-1}^n}{2(\Delta x^2)}+\frac{u_{i+1}^{n+1}-2u_i^{n+1}+u_{i-1}^{n+1}}{2(\Delta x^2)}-\alpha u_i^n. \tag{4.25}$$

Next, by substituting $u_i^n=\Psi(t)e^{j\gamma\Delta x}$ at time t where $j=\sqrt{(}-1)$ and $\gamma>0$, the method is shown to be stable by satisfying the following:

$$\left|\frac{\Psi(t+\Delta t)}{\Psi(t)}\right|\leq 1. \tag{4.26}$$

Substituting $u_i^n=\Psi(t)e^{i\gamma x}$ into (4.25), gives

$$\begin{aligned}\frac{\Psi(t+\Delta t)e^{j\gamma x}-\Psi(t)e^{j\gamma x}}{\Delta t}&=\frac{\Psi(t)e^{j\gamma(x+\Delta x)}-2\Psi(t)e^{j\gamma x}+\Psi(t)e^{j\gamma(x-\Delta x)}}{2\Delta x^2}\\&+\frac{\Psi(t+\Delta t)e^{j\gamma(x+\Delta x)}-2\Psi(t+\Delta t)e^{j\gamma x}+\Psi(t+\Delta t)e^{j\gamma(x-\Delta x)}}{2\Delta x^2}-\alpha\Psi(t)e^{j\gamma x}.\end{aligned} \tag{4.27}$$

Let $r=\Delta t/\Delta x^2$, so (4.27) simplifies to

$$\begin{aligned}\Psi(t+\Delta t)e^{j\gamma x}-\Psi(t)e^{j\gamma x}&=r\left(\frac{\Psi(t)e^{j\gamma(x+\Delta x)}-2\Psi(t)e^{j\gamma x}+\Psi(t)e^{j\gamma(x-\Delta x)}}{2}\right)\\&+r\left(\frac{\Psi(t+\Delta t)e^{j\gamma(x+\Delta x)}-2\Psi(t+\Delta t)e^{j\gamma x}+\Psi(t+\Delta t)e^{j\gamma(x-\Delta x)}}{2}\right)-\Delta t\alpha\Psi(t)e^{j\gamma x}.\end{aligned} \tag{4.28}$$

Note the $e^{j\gamma x}$ in all our terms. Dividing it out ,moving all the $\Psi(t+\Delta t)$ to the left of the equation, and all the $\Psi(t)$ to the right (4.28) takes the form

$$\begin{aligned}\Psi(t+\Delta t)-r\left(\frac{\Psi(t+\Delta t)e^{j\gamma\Delta x}-2\Psi(t+\Delta t)+\Psi(t+\Delta t)e^{-j\gamma\Delta x}}{2}\right)\\=r\left(\frac{\Psi(t)e^{j\gamma\Delta x}-2\Psi(t)+\Psi(t)e^{-j\gamma\Delta x}}{2}\right)+\Psi(t)-\Delta t\alpha\Psi(t).\end{aligned} \tag{4.29}$$

Factoring out common terms and simplifying gives

$$\Psi(t+\Delta t)\left(1-r\left(\frac{e^{j\gamma\Delta x}-2+e^{-j\gamma\Delta x}}{2}\right)\right)=\Psi(t)\left(r\left(\frac{e^{j\gamma\Delta x}-2+e^{-j\gamma\Delta x}}{2}\right)+1-\Delta t\alpha\right). \tag{4.30}$$

Using the following identity $\cos(u) = \frac{e^{jx}+e^{-jx}}{2}$, (4.30) takes the following form:

$$\Psi(t+\Delta t)\left(1 - r\left(\cos(\gamma\Delta x) - 1\right)\right) = \Psi(t)\left(r\left(\cos(j\gamma\Delta x) - 1\right) + 1 - \Delta t\alpha\right). \tag{4.31}$$

Applying $1 - \cos(2u) = 2\sin^2(u)$ yields

$$\Psi(t+\Delta t)\left(1 + 2r\sin^2(\frac{\gamma\Delta x}{2})\right) = \Psi(t)\left(1 - 2r\sin^2(\frac{\gamma\Delta x}{2}) - \Delta t\alpha\right). \tag{4.32}$$

It can be shown from (4.32) that,

$$\frac{\Psi(t+\Delta t)}{\Psi(t)} = \frac{1 - 2r\sin^2(\frac{\gamma\Delta x}{2}) - \Delta t\alpha}{1 + 2r\sin^2(\frac{\gamma\Delta x}{2})}. \tag{4.33}$$

Since

$$\left|\frac{1 - 2rsin^2(\frac{\gamma\Delta x}{2}) - \Delta t\alpha}{1 + 2rsin^2(\frac{\gamma\Delta x}{2})}\right| \leq 1. \tag{4.34}$$

Therefore, we have shown the psuedo-CN method is stable for sufficiently small Δt.

4.4 . DERIVATION OF PSUEDO-CRANK-NICOLSON SCHEME

To begin are implementation of the psuedo-CN method, the following partial derivatives are used [5]:

$$u(x_i, t_n) = u_i^n, \tag{4.35}$$

$$\frac{\partial u}{\partial t}(x_i, t_n) = \frac{u_i^{n+1} - u_i^n}{\Delta t}, \tag{4.36}$$

and

$$\frac{\partial^2 u}{\partial^2 x}(x_i, t_n) = \frac{1}{2}\left(\frac{u_{i+1}^{n+1} - 2u_i^{n+1} + u_{i-1}^{n+1}}{\Delta x^2} + \frac{u_{i+1}^n - 2u_i^n + u_{i-1}^n}{\Delta x^2}\right). \tag{4.37}$$

Here a forward approximation for the time derivative and an average between a forward and backward approximation for the second order spatial derivative is used. We now substitute (4.35), (4.36), and (4.37) into (2.1). This yields

$$\frac{u_i^{n+1} - u_i^n}{\Delta t} = \frac{1}{2\Delta x^2}(u_{i+1}^{n+1} - 2u_i^{n+1} + u_{i-1}^{n+1}) + \frac{1}{2\Delta x^2}(u_{i+1}^n - 2u_i^n + u_{i-1}^n)) + u_i^n(1 - u_i^n)(u_i^n - \alpha). \tag{4.38}$$

Next, multiply everything by Δt. This gives

$$u_i^{n+1} - u_i^n = \frac{\Delta t}{2\Delta x^2}(u_{i+1}^{n+1} - 2u_i^{n+1} + u_{i-1}^{n+1}) + \frac{\Delta t}{2\Delta x^2}(u_{i+1}^n - 2u_i^n + u_{i-1}^n)) + \Delta t u_i^n(1 - u_i^n)(u_i^n - \alpha). \tag{4.39}$$

To simplify our scheme, we will introduce the variable r and set $r = \frac{2\Delta t}{\Delta x^2}$. (4.39), then takes the form:

$$u_i^{n+1} - u_i^n = r(u_{i+1}^{n+1} - 2u_i^{n+1} + u_{i-1}^{n+1}) + r(u_{i+1}^n - 2u_i^n + u_{i-1}^n)) + \Delta t u_i^n(1 - u_i^n)(u_i^n - \alpha). \tag{4.40}$$

We can then move all the $n+1$ terms to the left hand side of the equation and move the n terms to the right. This gives (4.40) as

$$-ru_{i+1}^{n+1} + (2r+1)u_i^{n+1} - ru_{i-1}^{n+1} = r(u_{i+1}^n + u_{i-1}^n) + (1-2r)u_i^n + \Delta t u_i^n(1 - u_i^n)(u_i^n - \alpha). \tag{4.41}$$

Then (4.41) can be written in a matrix equation as

$$\mathbf{AU} = \mathbf{F}, \tag{4.42}$$

where the left hand side of the equation is a tri-diagonal matrix

$$A = \begin{pmatrix} (2r+1) & -r & 0 & \cdots & 0 \\ -r & (2r+1) & -r & \cdots & 0 \\ 0 & -r & (2r+1) & \ddots & 0 \\ \vdots & \vdots & \ddots & \ddots & -r \\ 0 & 0 & 0 & -r & (2r+1) \end{pmatrix}, \tag{4.43}$$

and the right side is

$$F = \begin{pmatrix} 0 \\ \vdots \\ r(u_{i+1}^n + u_{i-1}^n) + (1-2r)u_i^n + \Delta t u_i^n(1 - u_i^n)(u_i^n - \alpha) \\ \vdots \\ 1 \end{pmatrix}. \tag{4.44}$$

Therefore, we can find our solutions to the Nagumo equation using

$$\mathbf{U} = \mathbf{F}/\mathbf{A}. \tag{4.45}$$

CHAPTER V

NUMERICAL EXAMPLES

In this section, we are going to find the numerical values obtained by the (4.41). Then check the efficiency of our code by comparing the numerical values with the exact solution by Kawahara and Tanaka [13]. From there, more examples are ran with varying initial conditions.

For our numerical example, the following form of the Nagumo equation with initial and boundary conditions was used:

$$u_t = u_{xx} + u(1-u)(u-\alpha), \quad x \in \Omega, t \in [0,T], \tag{5.46}$$

$$u(x,0) = u_0(x), \ x \in \Omega, \tag{5.47}$$

$$\lim_{x_L \to -\infty} u(x_L,t) = 0, \lim_{x_R \to \infty} u(x_R,t) = 1, \quad t \in [0,T]. \tag{5.48}$$

5.1 . NUMERICAL SOLUTIONS TO THE NAGUMO EQUATION WITH EXACT SOLUTION

In our first example, a comparison between the pseudo-CN scheme to the exact solution of Kawahara and Tanaka [13] is examined. The exact solution of Kawahara and Tanaka is,

$$u(x,t) = \frac{Ae^{\Gamma_1} + \alpha B e^{\Gamma 2}}{Ae^{\Gamma_1} + Be^{\Gamma 2} + 1}, \tag{5.49}$$

with

$$\Gamma_1 = (\pm\sqrt{2}x + (1-2\alpha)t)/2,$$
$$\Gamma_2 = (\pm\sqrt{2}\alpha x + \alpha(\alpha-2)t)/2,$$

where A, B, and C are arbitrary constants. The $\pm$ is due to the Nagumo equation having two traveling waves as the solution, $+$ for right traveling wave and $-$ for left traveling wave.

For the numerical scheme, the arbitrary constants are equal to 1, consider right traveling waves, and the initial condition is defined as

$$u_0(x) = \frac{e^{\sqrt{2}x/2} + \alpha e^{\sqrt{2}\alpha x/2}}{e^{\sqrt{2}x/2} + e^{\sqrt{2}\alpha x/2} + 1}. \tag{5.50}$$

An approximate solution to our example with initial condition (5.50) is computed using finite difference method with $\Omega = [-100, 100]$ where $0 \le t \le 1$ (see Figure 5.1 and Figure 5.2). The maximum error

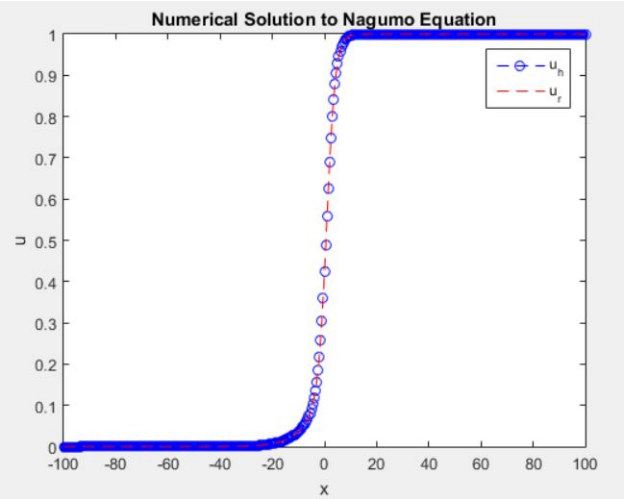

FIGURE 5.1. *Graph of u_r with $t = 1$.*

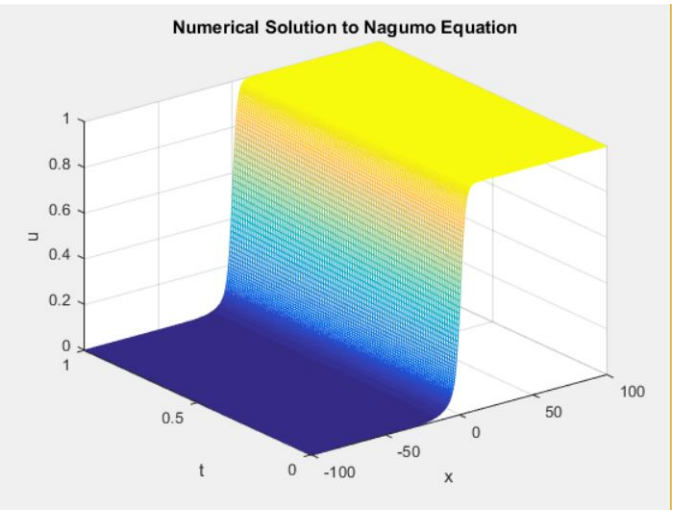

FIGURE 5.2. *Numerical solution of Nagumo Equation for $0 \leq t \leq 1$.*

was found using

$$\|u_h - u_r\|_{max} = \max_{0 \leq i \leq N} |u_h(x_i, t) - u_r(x_i, t)| \quad \text{at} \quad t = 0.1, \tag{5.51}$$

where u_h is the numerical result and u_r is the exact solution.

In Tables 5.1 and Table 5.2, numerical results for a range of values of Δt and Δx are presented. The errors are in the lower half of the table and the rates of convergence in the upper half. We can see from the data, that the maximum error for both fixed Δt and Δx ranges from 10^{-5} to 10^{-7}. This means that finer mesh results in a smaller maximum error. In Table 5.1, we see that at $t = 0.1$ and varying Δx, the

TABLE 5.1. *Maximum error and convergence rate with fixed Δt for $t = 0.1$.*

Spatial step, Δx	Δt =2e-05	Δt =4e-05	Δt =6e-05	Δt =8e-05
0.5	1.991	1.990	1.990	1.989
0.25	1.991	1.991	1.991	1.991
0.125	1.970	1.968	1.967	1.967
0.0625	1.883	1.885	1.885	1.885
0.5	3.065e-05	1.554e-05	1.041e-05	7.824e-05
0.25	7.712e-06	3.912e-06	2.621e-06	1.9702e-06
0.125	1.941e-06	9.845e-07	6.596e-07	4.958e-06
0.0625	4.955e-07	2.517e-07	1.687e-07	1.268e-07

TABLE 5.2. *Maximum error and convergence rate with fixed Δx.*

Time step Δt	$\Delta x = 0.5$	$\Delta x = 0.25$	$\Delta x = 0.125$	$\Delta x = 0.0625$
2e-05	0.993	0.993	1.001	1.030
4e-05	0.987	0.990	1.002	1.050
6e-05	0.982	0.986	1.003	1.070
8e-05	0.977	0.982	1.005	1.090
2e-05	6.608e-06	1.580e-06	3.973e-07	1.016e-07
4e-05	1.247e-05	3.144e-06	7.953e-07	2.075e-07
6e-05	1.861e-05	4.697e-06	1.194e-07	3.177e-07
8e-05	2.469e-05	6.238e-06	1.594e-06	4.322e-07

convergence rate was near two. The convergence rate for fixed spatial step and varying temporal steps in Table 5.2 are around one. This verifies the efficiency of our numerical scheme.

5.2 . PIECEWISE CONSTANT FUNCTION-ONE PULSE

In this section, the numerical scheme (4.41) can be used to solve more general problems of the Nagumo equation. The different simulations use different values for $u(x, 0)$, which is the height of the impulse. The efficiency of the pseudo-CN method used in the previous example simulates the different models, as long as the initial and boundary conditions are satisfied.

For the following examples, $\Delta x = \frac{25}{64}$ for the domain. This corresponds to the domain being partitioned into 512 pieces. The time step $\Delta t = 0.05$, gives a better history of the traveling wave. In all the examples, $\Omega = [-100, 100]$ where $0 \leq t \leq [0, 30]$, and the impulse length, x =[-L,L], for L = 5 and L=10.

In these examples, we will consider using a piecewise constant function with a impulse in the domain with an amplitude less than, equal to, and greater than α. The different amplitudes and lengths will give interesting results, especially considering α is unstable.

5.2 .1. CASE I

Let us consider a rectangular pulse with amplitude $u(x, 0) < \alpha$. Let

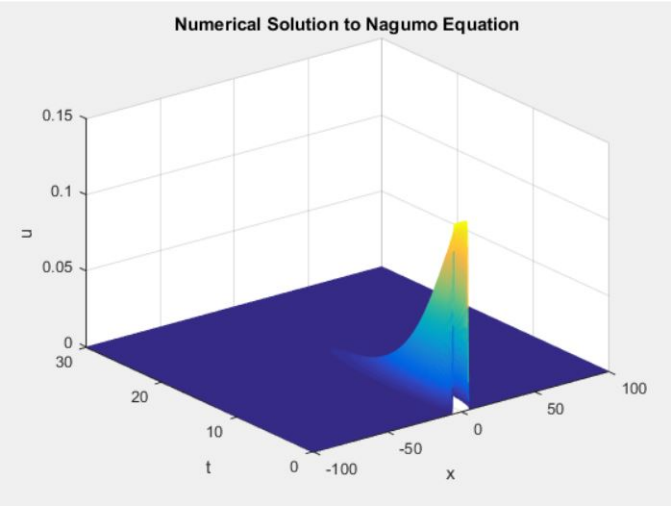

FIGURE 5.3. *Numerical solutions of Case I with impulse length from* $x = [-5, 5]$ *and* $u(x, 0) = \frac{\alpha}{2}$, *where* $0 \leq t \leq 30$.

$$u_0 = \begin{cases} 0 & \text{if } x < -L; \\ \frac{\alpha}{2} & \text{if } -L \leq x < L; \\ 0 & \text{if } x > L. \end{cases}$$

Figure 5.3 and Figure 5.4 are the corresponding graphs to this initial condition.

The two different length sizes for the rectangular impulses resulted in the same occurrence. Regardless of length $x = [-L, L]$, as long as the initial impulse amplitude was less than α the impulse damped out to the 0 rest state.

5.2 .2. CASE II

For this case, we will consider when the amplitude of our impulse is equal to the threshold α. This gives

$$u_0 = \begin{cases} 0 & \text{if } x < -L; \\ \alpha & \text{if } -L \leq x < L; \\ 0 & \text{if } x > L. \end{cases}$$

where the lengths of the impulses are $x = [-5, 5]$ and $x = [-10, 10]$. The impulses with an amplitude of α, resulted in damping down to the 0 resting state. This is shown in Figure 5.5 and Figure 5.6.

To show that the length of the impulse does not determine the steady state the impulse approaches, set $x = [-50, 50]$ and our time domain increased to $T = 90$, as displayed in Figure 5.7. The impulse still damped down to the resting state.

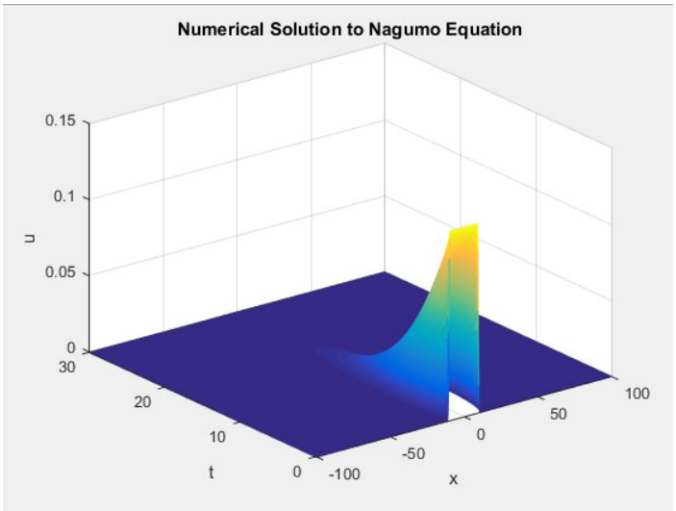

FIGURE 5.4. *Numerical Solution of Case I with impulse length from* $x = [-10, 10]$ *and* $u(x, 0) = \frac{\alpha}{2}$, *where* $0 \leq t \leq 30$.

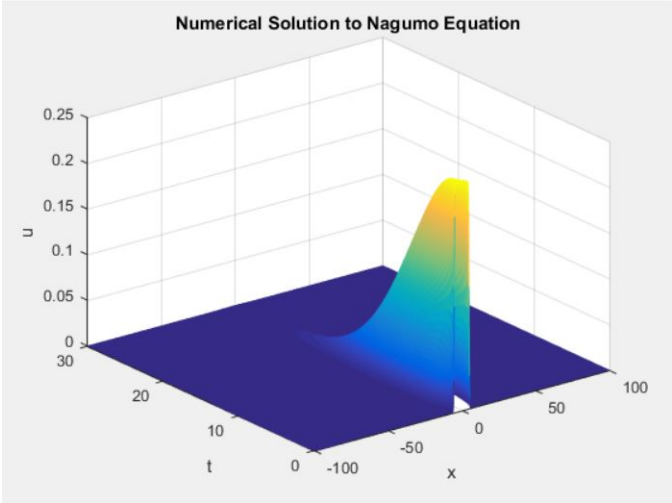

FIGURE 5.5. *Numerical solutions of Case II with impulse length from* $x = [-5, 5]$ *and* $u(x, 0) = \alpha$, *where* $0 \leq t \leq 30$.

5.2 .3. CASE III

For this case we are considering, an impulse pulse with $u(x, 0) > \alpha$ for $x = [-5, 5]$ and $x = [-10, 10]$. Let

$$u_0 = \begin{cases} 0 & \text{if } x < -L; \\ \frac{3\alpha}{2} & \text{if } -L \leq x < L; \\ 0 & \text{if } x > L. \end{cases}$$

The initial impulses with amplitude larger than α should results in the impulse growing to the 1 excited state. The impulse, regardless of length, will go to the rest state 1 as $t \to \infty$, since $u(x, 0) > \alpha$. The results of our simulations can be seen in Figure 5.8, Figure 5.9, and Figure 5.10.

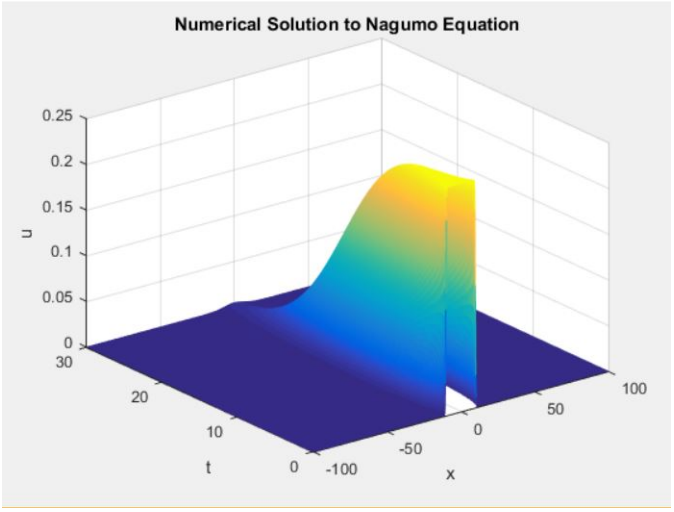

FIGURE 5.6. *Numerical solutions of Case II with impulse length from* $x = [-10, 10]$ *and* $u(x, 0) = \alpha$*, where* $0 \leq t \leq 30$.

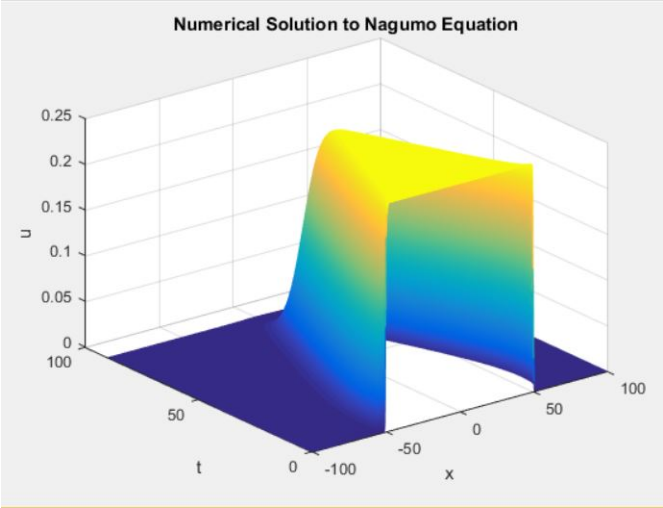

FIGURE 5.7. *Numerical solutions of Case II with impulse length from* $x = [-50, 50]$ *and* $u(x, 0) = \alpha$*, where* $0 \leq t \leq 90$.

In this example, the impulse size does not have an effect on the steady state the solution will converge to. The model behaves similar to the HH model and FN model in the sense that it requires a threshold voltage to simulate an action potential. In summary, if the $u(x, 0) \leq \alpha$ are solution will converge to the rest state 0. If the $u(x, 0) > \alpha$, then we will have a solution that goes to the rest state 1 as $t \to \infty$. The purpose of this example, was to simulate the all or none principle associated with an action potential model.

5.3 . PIECEWISE CONSTANT FUNCTION-TWO PULSE

In the previous section, the focus was on one impulse with varying lengths. The results confirmed the amplitude governed the steady state the impulse would approach as $t \to \infty$ and the length of the impulse

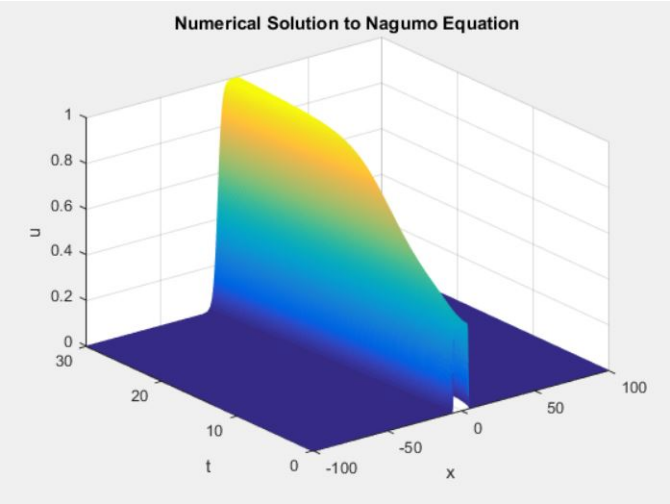

FIGURE 5.8. *Numerical solutions of Case II with impulse length from* $x = [-5, 5]$ *and* $u(x, 0) = \frac{3\alpha}{2}$, *where* $0 \leq t \leq 30$.

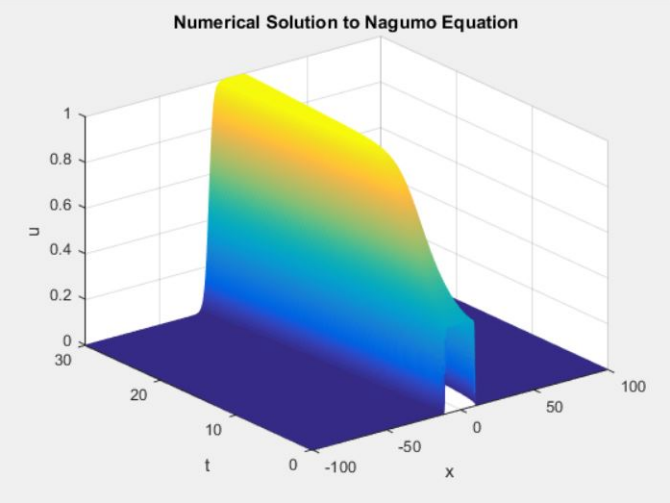

FIGURE 5.9. *Numerical solutions of Case II with impulse length from* $x = [-10, 10]$ *and* $u(x, 0) = \frac{3\alpha}{2}$, *where* $0 \leq t \leq 30$.

had no effect.

In this section the numerical results involve two impulses with varying amplitudes. Since the length of the impulse did not govern which steady state the impulse approached, the length of the impulses would be both equal to 50. The main result we want to show is if two impulses with a combined amplitude greater than α would have the same result as one impulse with amplitude greater than α. For example, if the two impulses amplitude is greater than α, then it should model the same behavior as one impulse greater than α did. Similarly for the other two cases when their amplitudes are equal to α and less than α. For these cases, the domain is $\Omega[-100, 100]$ and $0 \leq t \leq 30$.

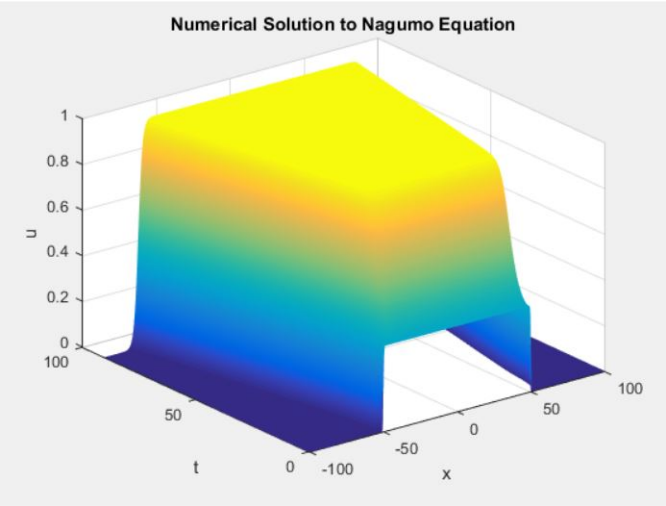

FIGURE 5.10. *Numerical solutions of Case III with impulse length from* $x = [-50, 50]$ *and* $u(x, 0) = \frac{3\alpha}{2}$, *where* $0 \leq t \leq 90$.

5.3 .1. CASE I

The first case we will consider when both amplitudes combined is less than α. Let

$$u_0 = \begin{cases} 0 & \text{if } x < -\frac{3}{4}L; \\ 0.2 & \text{if } -\frac{3}{4}L \leq x < -\frac{1}{4}L; \\ 0 & \text{if } -\frac{1}{4}L \leq x < \frac{1}{4}L; \\ 0.2 & \text{if } \frac{1}{4}L \leq x < \frac{3}{4}L; \\ 0 & \text{if } x > \frac{3}{4}L. \end{cases}$$

In this simulation, both impulses with amplitudes less than α damped down to the 0 resting state. Even though, the combined amplitudes of both impulses is greater than α the result is similar to one pulse. Figure 5.3 .1 shows our simulation results.

5.3 .2. CASE II

For this case, we will consider

$$u_0 = \begin{cases} 0 & \text{if } x < -\frac{3}{4}L; \\ 0.2 & \text{if } -\frac{3}{4}L \leq x < -\frac{1}{4}L; \\ 0 & \text{if } -\frac{1}{4}L \leq x < \frac{1}{4}L; \\ \frac{3}{4}\alpha & \text{if } \frac{1}{4}L \leq x < \frac{3}{4}L; \\ 0 & \text{if } x > \frac{3}{4}L. \end{cases}$$

In this simulation we got the same results as before when we had one impulse's amplitude equal to α. As long as one impulse is larger than the threshold value, α, it will rise to the 1 excited state. This is

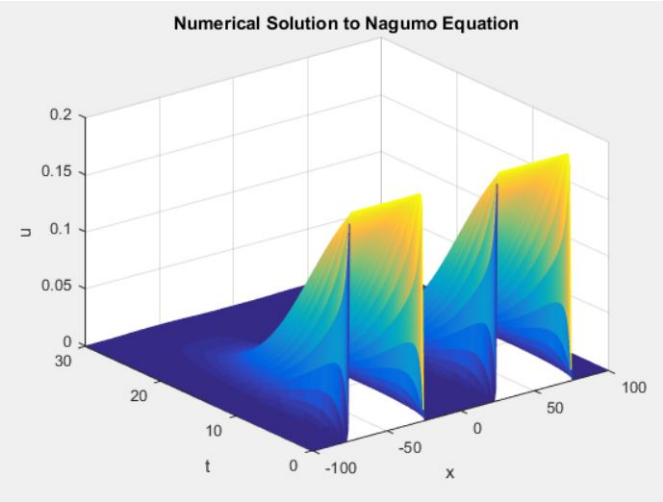

FIGURE 5.11. *Numerical solutions of Case I with two impulses and* $u(x,0) = 0.2$*, where* $0 \leq t \leq 30$.

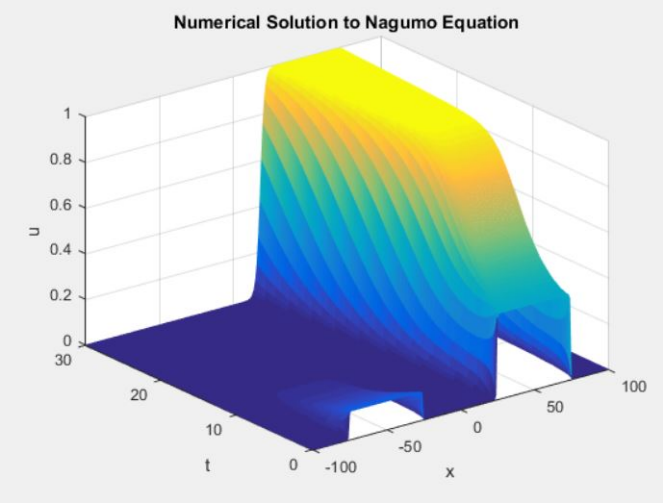

FIGURE 5.12. *Numerical solutions of Case II with impulse one's* $u(x,0) = 0.2$ *and impulse two's* $u(x,0) = \frac{3}{2}\alpha$*, where* $0 \leq t \leq 30$.

displayed in Figure 5.12.

5.3 .3. CASE III

We will now simulate, what will happen when our two impulses have an amplitude greater than α. Let

$$u_0 = \begin{cases} 0 & \text{if } x < -\frac{3}{4}L; \\ \frac{3}{2} & \text{if } -\frac{3}{4}L \leq x < -\frac{1}{4}L; \\ 0 & \text{if } -\frac{1}{4}L \leq x < \frac{1}{4}L; \\ \frac{3}{2} & \text{if } \frac{1}{4}L \leq x < \frac{3}{4}L; \\ 0 & \text{if } x > \frac{3}{4}L. \end{cases}$$

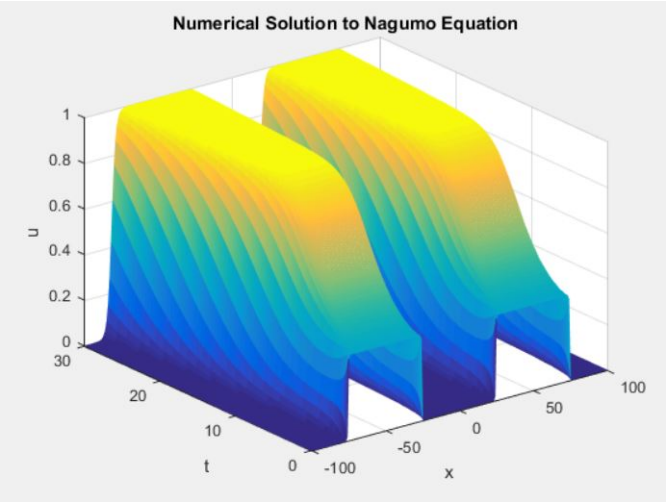

FIGURE 5.13. *Numerical solutions of Case III with two impulses with* $u(x,0) = \frac{3}{2}\alpha$*, where* $0 \leq t \leq 30$.

This simulation had interesting results. When comparing it to the previous simulation, this case went to the 1 excited state at a faster rate. Though, the amplitude of the impulse governs which steady state the impulse approaches, the number of impulses with amplitudes greater than α increases the rate at which it reaches the excited state. As seen in Figure 5.13

CHAPTER VI

CONCLUSION

The Nagumo equation is one of the most researched models of the action potential. Due to the nonlinearity of the equation, the numerical solutions yielded interesting results. In this thesis, it was shown that the Nagumo equation can give traveling wave solutions (see also [7], [12], [20], and [23]), as well as model the all or none principle seen in the HH model and FN model. Once the efficiency of the numerical scheme was verified different cases involving varying lengths, amplitudes, amount of the impulses were carried out. It was shown that the governing factor in determining the state at which the impulse goes to was the amplitude, and that the length of the impulse did not matter. The interesting result was that the more impulses with amplitude greater than α increased the rate at which the impulse would reach the excited state.

Future work would be to solve the Nagumo Equation using the finite element method, then compare the results with the finite difference method used in this thesis. Other additional work would be to find numerical solutions to additional reaction-diffusion equations similar to the Nagumo equation, but differing in the nonlinear term $f(u)$.

REFERENCES

[1] D. G. ARONSON, H. F. WEINBERGER, *Nonlinear diffusion in population genetics, combustion, and nerve propagation*, Partial Differential Equations and Related Topics, Lecture Notes in Math. 446, Springer, New York, 1975, pp. 5 - 49.

[2] N. F. BRITTON, *Reaction-Diffusion Equations and their Applications to Biology*, Academic Press, London, 1986.

[3] P. BROWNE, E. MOMONIAT, R. M. MAHOMED, *A generalized Fitzhugh-Nagumo Equation*, Nonlinear Analysis, 68 (2008), pp. 1006-1015.

[4] K. S. COLE, H. J. CURTIS, *Electrical impedence of the squid axon during activity*, Journal of General Physiology, 22 (1939), pp. 649-670.

[5] G. EVANS, J. BLACKLEDGE, P. YARDLEY, *Numerical Methods for Partial Differential Equations*, Springer, London, 2000.

[6] S. E. FADUGBA, O. H. EDOGBANYA, S. C. ZELIBE, *Crank Nicolson method for solving parabolic partial differential equations*, International Journal of Applied Mathematics and Modeling, 1 (3) (2013) 8-23.

[7] P. C. FIFE, J. B. MCLEOD, *The approach of solutions of nonlinear diffusion equations to travelling wave solutions*, Bulletin of the American Mathematical Society, 81 (6) (1975), pp. 1076-1078.

[8] R. FITZHUGH, *Impulse and physiological states in models of nerve membranes*, Biophys. J., 1 (1961), pp. 445-466.

[9] R. FITZHUGH, *Mathematical models of excitation and propagation in nerve*. Chapter 1 (pp. 1-85 in H.P. Schwan, ed. Biological Engineering, McGraw-Hill Book Co., N.Y. 1969).

[10] M. W. GREEN, B. D. SLEEMAN, *On FitzHugh's nerve axon equations*, J. Math. Biology, 1 (1974), pp. 153163.

[11] A. L. HODGKIN, A. F. HUXLEY, *A quantitative description of membrane current and its applications to conduction and excitation in nerve*, The Journal of physiology, 117 (4) (1952), pp. 500-544.

[12] M. IQBAL, *Numerical Solutions of Nagumo's equation*, Journal of Applied Mathematics and Decision Sciences, 3 (2) (1999), pp. 189-193.

[13] T. KAWAHARA, M. TANAKA, *Interactions of travelling fronts: an exact solution of a nonlinear diffusion equation*, Phys. Lett. A, 97 (1983), pp. 311-314.

[14] H. LI, Y. GUO, *New exact solutions to the Fitzhugh-Nagumo equation*, Applied Mathematics and Computation, 180 (2006), pp. 524-528.

[15] S. A. MANAA, M. A. MOHEEMMEED, *Numerical solution and stability analysis of Huxley equation*, Raf. J. of Comp. and Math., 2 (1) (2005), pp. 85-97.

[16] H. K. MCKEAN, *Nagumo's equation*, Advances in Mathematics, 4 (1970), pp. 209-223.

[17] J. MURRAY, *Mathematical Biology I: An Introduction*, Springer, N. Y., 2002.

[18] J. S. NAGUMO, S. ARIOMOTO, S. YOSHIZAWA, *An active pulse transmission line simulatiing nerve axon*, Proc. of the IRE, 50 (1962), pp. 2061-2070.

[19] J. S. NAGUMO, S. ARIOMOTO, S. YOSHIZAWA, *Bistable transmission lines*, I.E.E.E. Transactions on Circuit Theory, 12 (1965), pp. 400-412.

[20] J. RINZEL, J. KELLER, *Traveling Wave Solutions of a Nerve Conduction Equation*, Biophys. J., 13 (1973), pp. 975 - 988.

[21] S. SCHUETZE, *The discovery of the action potential, Trends in Neurosciences*, 83 (1983), pp. 164-168.

[22] T. TRAPPENBERG, *Fundamentals of Computational Neuroscience*, Oxford University Press, N.Y., 2002.

[23] B. ZINNER, *Existence of Traveling Wavefront Solutions for the Discrete Nagumo Equation*, Journal of Differential Equation, 96 (1992), pp. 1-27.

APPENDIX A

HODGKIN-HUXLEY MATLAB CODE

HODGKIN-HUXLEY MATLAB CODE

```
%Hodgkin-Huxley - Forward Euler Method
%Simulation Time
time = 100; %milliseconds
dt=0.001;
t=0:dt:time;

%Stimulus
Iapp = [10];
%Set outside stimulus I_applied
I(1:numel(t)) = Iapp;

%Resting Potential
V=-70;

%parameters of the Hodgkin-Huxley equations
gbarK=36; gbarNa=120; g_L=.3;    %mS/cm^2
E_K = -12; E_Na=115; E_L=10.6;   %milliVolts
C=1;                             %membrane capacity, muF/cm^2

%rate constants( alpha and beta)
alpha_n = 0.01*(-V+10)/(exp(1-(0.1*V))-1);
beta_n  = 0.125*exp(-V/80.0);
alpha_m = .1*(25-V) / (exp(2.5-0.1*V)-1);
beta_m  = 4*exp(-V/18);
alpha_h = .07*exp(-V/20);
beta_h  = 1/(exp(3-0.1*V)+1);

%steady state values of n,m,h with membrane potential at resting potential
n(1) = alpha_n/(alpha_n+beta_n);
m(1) = alpha_m/(alpha_m+beta_m);
h(1) = alpha_h/(alpha_h+beta_h);

%calculate new values
for i=1:numel(t)-1 %time steps

    %Calculate alpha and beta
    %Equations here are same as above, just calculating at each time step
    alpha_n(i) = .01 * ( (10-V(i)) / (exp((10-V(i))/10)-1) );
    beta_n(i) = .125*exp(-V(i)/80);
    alpha_m(i) = .1*( (25-V(i)) / (exp((25-V(i))/10)-1) );
    beta_m(i) = 4*exp(-V(i)/18);
    alpha_h(i) = .07*exp(-V(i)/20);
    beta_h(i) = 1/(exp((30-V(i))/10)+1);
```

```
    %Calculate Ion currents%
    I_Na = (m(i)^3) * gbarNa * h(i) * (V(i)-E_Na);
    I_K = (n(i)^4) * gbarK * (V(i)-E_K);
    I_L = g_L *(V(i)-E_L);
    I_ion = I(i) - I_K - I_Na - I_L;

    %Euler First Order Approximation to find new voltage%
    V(i+1) = V(i) + dt*I_ion/C;
    n(i+1) = n(i) + dt*(alpha_n(i) *(1-n(i)) - beta_n(i) * n(i));
    m(i+1) = m(i) + dt*(alpha_m(i) *(1-m(i)) - beta_m(i) * m(i));
    h(i+1) = h(i) + dt*(alpha_h(i) *(1-h(i)) - beta_h(i) * h(i));
end
%Plot Voltage
figure
plot(t,V,'LineWidth',3)
hold on
legend({'voltage'})
ylabel('Voltage (mv)')
xlabel('time (ms)')
title('Voltage over Time in Simulated Neuron with I_applied=')
%Gating Variable, n(t), m(t), h(t)
figure
p1 = plot(t,m,'LineWidth',2);
hold on
p2 = plot(t,n,'r','LineWidth',2);
hold on
p3=plot(t,h,'g','LineWidth',2);
legend([p1, p2, p3], 'm(t), Potassium Activation', 'n(t), Sodium Activation','h(t),
ylabel('Gating Variables')
xlabel('time (ms)')
title('Activation and Deactivation of Gating Variables')
```

APPENDIX B

FITZHUGH-NAGUMO MATLAB CODE

FITZHUGH-NAGUMO MATLAB CODE

```
%Fitzhugh Nagumo - Forward Euler Method

%Simulation Time
time = 100; %milliseconds
dt=0.001;
t=0:dt:time;

%Stimulus
I = [1];

%Set initial conditions
Vo = -1.5;%-1.1994;
Wo = -3/8;%-0.6243;
V=Vo; W=Wo;
%calculate new values
for i=1:numel(t)-1 %time steps

    %Euler First Order Approximation to find new voltage%
    V(i+1) = (dt+1).*V(i) + dt.*(I - (V(i).^3)./3 - W(i));
    W(i+1) = (1-0.08*0.8*dt).*W(i)+dt*0.08.*(V(i)+0.7);
end

%Plot Voltage
figure
p1 = plot(t,V,'LineWidth',3);
hold on
p2 = plot(t,W,'LineWidth',2);
legend([p1, p2], 'V(t), voltage variable', 'W(t), recovery variable')
ylabel('Voltage (mv)')
xlabel('time (ms)')
title('Voltage over Time in Simulated Neuron with I =')
```

APPENDIX C

MATLAB CODE FOR EXAMPLES 1, 2, AND 3

NAGUMO EQUATION MATLAB CODE FOR EXAMPLES 1, 2, AND 3

```
%Nagumo Equation- Crank-Nicolson Method
%u_t = u_xx - u*(1-u)(u-a)
%for 0 < a < 0.5

%Domain x in [-L,L]
L = 100;

% Define parameters
alpha = .25;
dt= .05;%time step
tlp = 600;%time to be 30 seconds tlp/dt = 30.
N = 200;%Partition
dx =2*L/N;%Step size
r =  dt/(2*dx^2);
x =  -L:dx:L;
n2= N+1;

uGd = [];

u0 = zeros(N+1,1);
%Example 1: Initial condition, u(x,0) = u0(x)
t = 0;
     gamma1 = sqrt(2)/2.*x + (0.5 - alpha).*t;
     gamma2 = sqrt(2)/2.*alpha.*x + alpha.*(alpha - 2).*t/2;
u0(1:n2) = (exp(gamma1) + alpha.*exp(gamma2))./(exp(gamma1)+exp(gamma2)+1);

%Example 2: Initial conditons
%minV = N/2+1 - 250;
%maxV = N/2+1 + 250;
%for j = 1:n2
%    if j < minV
%        u0(j) = 0;
%    elseif j >=minV && j<maxV
%        u0(j) = 3*alpha/2;% alpha;%alpha/2;
%    elseif j >= maxV
%        u0(j)=0;
%    end
%end

%Example 3: Initial conditons
%nminV = N/2+1 -100;
%nmaxV = N/2+1 - 50;
%pminV = N/2+1 + 50;
%pmaxV = N/2+1 + 100;
```

```
%shift=49.5;% changes the spacing inbetween the two impulses
%for j = 1:n2
 %   if j < nminV+shift
%        u0(j) = 0;
%    elseif j >=nminV+shift && j<nmaxV+shift
%        u0(j) = .20;% alpha;%alpha/2;
%    elseif j>=nmaxV+shift && j<pminV-shift
%        u0(j) = 0;
%    elseif j>=pminV-shift && j<pmaxV-shift
%        u0(j)  = 3*alpha/2;%alpha/2;
%    elseif j >= pmaxV-shift
%        u0(j)=0;
%    end
%end

%initial time step
u1 = u0;
 for j = 1:  tlp
     %Stiffness matrix
   A =    diag([1, (2*r  + 1) * ones(1,N-1) ,1])...
        + diag([(-r)*ones(1,N-1) , 0]                        ,-1)...
        + diag([                   0 ,  (-r)*ones(1,N-1)],1);
    %Load vectore
   F = (1 - 2*r)* u1 + r * ([0 ;u1(1:N)]...
        + [u1(2:N+1);1]) + dt .* (u1).*(1-u1).*(u1-alpha);

    F(1)=0;
    F(N+1)=1;
    uh = A\F;
    %Corresponds to next time step
    u1=uh;
    uGd = [uGd, uh ];

   %Example 1 exact solution% for the other examples comment out the exact solution
    tf = j*dt;
    gamma1 = sqrt(2)/2.*x + (0.5 - alpha).*tf;
    gamma2 = sqrt(2)/2.*alpha.*x + alpha.*(alpha - 2).*tf/2;
    ue = (exp(gamma1) + alpha.*exp(gamma2))./(exp(gamma1)+exp(gamma2)+1);
    uexact=ue';

    %Example 1 graph
    plot(x,uh,'b--o',x,ue,'r--')
    %Example 2 and 3 garphs
    %plot(x,uh)

    hold on
```

```
    ylabel('u')
    xlabel('x')
    axis([-L L 0 1])
    title('Numerical Solution to Nagumo Equation')
    hold off

 end
hold off

figure
[x,t] = meshgrid(-L:dx:L,(0:tlp)*dt);
mesh(x,t,uGd')
hold on
zlabel('u')
ylabel('t')
xlabel('x')
title('Numerical Solution to Nagumo Equation')
```

APPENDIX D

MATLAB CODE FOR CONVERGENCE RATE FOR FIXED SPATIAL STEP

```
%Nagumo Equation---Convergence rate fixed spatial and time discretization
%u_t = u_xx - u*(1-u)(u-a)
%for 0 < a < 0.5

%Domain x in [-L,L]
L = 100;

% Define parameters
alpha = .25;
Err = [];

k=1;
N =200*2^k;%Partition
dx =2*L/N;%Step size
%h(k)=dx;
tlp = 1000;
loop = 5;
x =  -L:dx:L;

for i=1:loop

dt= .00001*2*(i);%time step
tau(i)=dt;
r =  dt/(2*dx^2);

n2= N+1;

u0 = zeros(N+1,1);
%Simulation 1: Initial condition, u(x,0) = u0(x)
t = 0;
     gamma1 = sqrt(2)/2.*x + (0.5 - alpha).*t;
     gamma2 = sqrt(2)/2.*alpha.*x + alpha.*(alpha - 2).*t/2;
u0(1:n2) = (exp(gamma1) + alpha.*exp(gamma2))./(exp(gamma1)+exp(gamma2)+1);

%initial time step
u1 = u0;
 for j = 1:  tlp
     %Stiffness matrix
   A =    diag([1, (2*r  + 1) * ones(1,N-1) ,1])...
        + diag([(-r)*ones(1,N-1) , 0]                    ,-1)...
        + diag([                   0 ,  (-r)*ones(1,N-1)],1);
    %Load vectore
   F = (1 - 2*r)* u1 + r * ([0 ;u1(1:N)]...
        + [u1(2:N+1);1]) + dt .* (u1).*(1-u1).*(u1-alpha);
```

```
    F(1)=0;
    F(N+1)=1;
    uh = A\ F;
    %Corresponds to next time step
    u1=uh;

   %For Simulation 1 exact solution delete the %
    tf = j*dt;
    gamma1 = sqrt(2)/2.*x + (0.5 - alpha).*tf;
    gamma2 = sqrt(2)/2.*alpha.*x + alpha.*(alpha - 2).*tf/2;
    ue = (exp(gamma1) + alpha.*exp(gamma2))./(exp(gamma1)+exp(gamma2)+1);
    uexact=ue';

    plot(x,uh,'b--o',x,ue,'r--')
    legend('u_{num}','exact')
    hold on
    ylabel('u')
    xlabel('x')
    axis([-L L 0 1])
    title('Numerical Solution to Nagumo Equation')
%    pause
 hold off

 end
   %Finds the discrete maximum error of the numerical solution to each h
  Err=[Err,max(abs(uh-uexact))];
end
 %convergence rate of numerical scheme
rate =log(Err(1:loop-1)./Err(2:loop))./log(tau(1:loop-1)./tau(2:loop))
```

VITA

Gabriel Perry Natanni Garcia was born August 26, 1984 in Portales, New Mexico. He spent most of his life in Laredo, Texas. After graduating from United High School in 2002, he attended Laredo Community College before being enrolled at Texas A&M University in College Station from the 2006 to 2009. At Texas A&M, he was the secretary of the local Society of Physics Students and a member of the American Physics Society. He received his B.S. in Physics in 2009.

In the years after, he enrolled as a full-time student at Texas A&M International University pursuing a degree leading to M.S. in Mathematics, as well as a certification in teaching. As a full time student, he is also a high school mathematics teacher at Martin High School in Laredo, Texas. He has taught everything from Algebra to Precalculus. His interests are in mathematical modeling and he plans in the future to obtain a Ph. D. in Mathematics. He can be reached at 1918 Denmark Ln, Laredo, TX, 78045.